Dynamics of femtosecond laser-induced breakdown in water from femtoseconds to microseconds

Chris B. Schaffer,[*] Nozomi Nishimura,[†] Eli N. Glezer,[‡] Albert M.-T. Kim, and Eric Mazur

Harvard University, Department of Physics and Division of Engineering and Applied Sciences, Cambridge, MA 02138

chris_schaffer@post.harvard.edu, mazur@physics.harvard.edu

http://mazur-www.harvard.edu/

Abstract: Using time-resolved imaging and scattering techniques, we directly and indirectly monitor the breakdown dynamics induced in water by femtosecond laser pulses over eight orders of magnitude in time. We resolve, for the first time, the picosecond plasma dynamics and observe a 20 ps delay before the laser-produced plasma expands. We attribute this delay to the electron-ion energy transfer time.

OCIS codes: (140.3440) Laser-induced breakdown; (320.2250) Femtosecond phenomena; (190.7110) Ultrafast nonlinear optics

References and Links

1 K. Miura, J. R. Qiu, H. Inouye, T. Mitsuyu, and K. Hirao, "Photowritten optical waveguides in various glasses with ultrashort pulse laser," Appl. Phys. Lett. **71**, 3329 (1997).

2 D. Homoelle, S. Wielandy, A. L. Gaeta, N. F. Borrelli, and C. Smith, "Infrared photosensitivity in silica glasses exposed to femtosecond laser pulses," Opt. Lett. **24**, 1311 (1999).

3 E. N. Glezer, M. Milosavljevic, L. Huang, R. J. Finlay, T. H. Her, J. P. Callan, and E. Mazur, "Three-dimensional optical storage inside transparent materials," Opt. Lett. **21**, 2023 (1996).

4 C. B. Schaffer, A. Brodeur, J. F. Garcia, and E. Mazur, "Micromachining bulk glass by use of femtosecond laser pulses with nanojoule energy," Opt. Lett. **26**, 93 (2001).

5 T. Juhasz, H. Frieder, R. M. Kurtz, C. Horvath, J. F. Bille, and G. Mourou, "Corneal refractive surgery with femtosecond lasers," IEEE J. Sel. Top. Quantum Electron. **5**, 902 (1999).

6 F. H. Loesel, J. P. Fischer, M. H. Gotz, C. Horvath, T. Juhasz, F. Noack, N. Suhm, and J. F. Bille, "Non-thermal ablation of neural tissue with femtosecond laser pulses," Appl. Phys. B **66**, 121 (1998).

7 K. Konig, I. Riemann, and W. Fritzsche, "Nanodissection of human chromosomes with near-infrared femtosecond laser pulses," Opt. Lett. **26**, 819 (2001).

8 N. Shen, C. B. Schaffer, D. Datta, and E. Mazur, "Photodisruption in biological tissues and single cells using femtosecond laser pulses," in *Conference on Lasers and Electro-Optics* (Optical Society of America, Washington, DC, 2001), Vol. 56, p. 403 .

9 A. A. Oraevsky, L. B. DaSilva, A. M. Rubenchik, M. D. Feit, M. E. Glinsky, M. D. Perry, B. M. Mammini, W. Small, and B. C. Stuart, "Plasma mediated ablation of biological tissues with nanosecond-to-femtosecond laser pulses: Relative role of linear and nonlinear absorption," IEEE J. Sel. Top. Quantum Electron. **2**, 801 (1996).

10 E. N. Glezer and E. Mazur, "Ultrafast-laser driven micro-explosions in transparent materials," Appl. Phys. Lett. **71**, 882 (1997).

11 M. Lenzner, J. Kruger, S. Sartania, Z. Cheng, C. Spielmann, G. Mourou, W. Kautek, and F. Krausz, "Femtosecond optical breakdown in dielectrics," Phys. Rev. Lett. **80**, 4076 (1998).

12 D. Du, X. Liu, G. Korn, J. Squier, and G. Mourou, "Laser-induced breakdown by impact ionization in sio2 with pulse widths from 7 ns to 150 fs," Appl. Phys. Lett. **64**, 3071 (1994).

13 B. C. Stuart, M. D. Feit, S. Herman, A. M. Rubenchik, B. W. Shore, and M. D. Perry, "Optical ablation by high-power short-pulse lasers," J. Opt. Soc. Am. B **13**, 459 (1996).

14 B. C. Stuart, M. D. Feit, S. Herman, A. M. Rubenchik, B. W. Shore, and M. D. Perry, "Nanosecond-to-femtosecond laser-induced breakdown in dielectrics," Phys. Rev. B **53**, 1749 (1996).

15 C. B. Schaffer, A. Brodeur, and E. Mazur, "Laser-induced breakdown and damage in bulk transparent materials induced by tightly-focused femtosecond laser pulses," Meas. Sci. Technol. **12**, 1784 (2001).

[*] Current address: University of California, San Diego, Department of Chemistry and Biochemistry, La Jolla, CA 92093

[†] Current address: University of California, San Diego, Department of Physics, La Jolla, CA 92093

[‡] Current address: IGEN, Inc., Gaithersburg, MD 20877

#685 - $15.00 US Received December 19, 2001; Revised February 08, 2002

16 E. N. Glezer, C. B. Schaffer, N. Nishimura, and E. Mazur, "Minimally disruptive laser-induced breakdown in water," Opt. Lett. **22**, 1817 (1997).
17 A. G. Doukas, A. D. Zweig, J. K. Frisoli, R. Birngruber, and T. F. Deutsch, "Non-invasive determination of shock wave pressure generated by optical breakdown," Appl. Phys. B **53**, 237 (1991).
18 T. Juhasz, G. A. Kastis, C. Suarez, Z. Bor, and W. E. Bron, "Time-resolved observations of shock waves and cavitation bubbles generated by femtosecond laser pulses in corneal tissue and water," Laser Surg. Med. **19**, 23 (1996).
19 P. K. Kennedy, S. A. Boppart, D. X. Hammer, B. A. Rockwell, G. D. Noojin, and W. P. Roach, "A first-order model for computation of laser-induced breakdown thresholds in ocular and aqueous media .2. Comparison to experiment," IEEE J. Quantum Electron. **31**, 2250 (1995).
20 J. Noack, D. X. Hammer, G. D. Noojin, B. A. Rockwell, and A. Vogel, "Influence of pulse duration on mechanical effects after laser-induced breakdown in water," J Appl Phys **83**, 7488 (1998).
21 A. Vogel, J. Noack, K. Nahen, D. Theisen, S. Busch, U. Parlitz, D. X. Hammer, G. D. Noojin, B. A. Rockwell, and R. Birngruber, "Energy balance of optical breakdown in water at nanosecond to femtosecond time scales," Appl. Phys. B **68**, 271 (1999).
22 E. Abraham, K. Minoshima, and H. Matsumoto, "Femtosecond laser-induced breakdown in water: Time-resolved shadow imaging and two-color interferometric imaging," Opt. Commun. **176**, 441 (2000).
23 A. Vogel, K. Nahen, D. Theisen, R. Birngruber, R. J. Thomas, and B. A. Rockwell, "Influence of optical aberrations on laser-induced plasma formation in water and their consequences for intraocular photodisruption," Appl. Opt. **38**, 3636 (1999).
24 J. P. Fischer, T. Juhasz, and J. F. Bille, "Time resolved imaging of the surface ablation of soft tissue with ir picosecond laser pulses," Appl. Phys. A **64**, 181 (1997).
25 A. Vogel, S. Busch, and U. Parlitz, "Shock wave emission and cavitation bubble generation by picosecond and nanosecond optical breakdown in water," J. Acoust. Soc. Amer. **100**, 148 (1996).
26 J. G. Fujimoto, Ophthal. & Vis. Science **26**, 1771 (1985).
27 C. A. Puliafito and R. F. Steinert, IEEE J. Quantum Electron. **20**, 1442 (1984).
28 L. Huang, J. P. Callan, E. N. Glezer, and E. Mazur, "Gaas under intense ultrafast excitation: Response of the dielectric function," Phys. Rev. Lett. **80**, 185 (1998).
29 C. B. Schaffer, "Interaction of femtosecond laser pulses with transparent materials," Ph.D. thesis, Harvard University (2001).
30 D. von der Linde and H. Schuler, "Breakdown threshold and plasma formation in femtosecond laser-solid interaction," J. Opt. Soc. Am. B **13**, 216 (1996).
31 T. Juhasz, G. Djotyan, F. H. Loesel, R. M. Kurtz, C. Horvath, J. F. Bille, and G. Mourou, "Applications of femtosecond lasers in corneal surgery," Laser Phys. **10**, 495 (2000).

Introduction

Femtosecond laser-induced breakdown in transparent materials has attracted much attention in recent years. Nonlinear absorption of tightly-focused femtosecond laser pulses inside transparent materials creates a high-temperature plasma at the laser focus, providing an ideal means for the micromachining of bulk transparent materials [1-4], and offering a precise laser scalpel for photodisruptive surgery in both tissue and single cells [5-9]. Recent studies of laser-induced breakdown in solids have focused on absorption mechanisms, threshold dependencies on pulsewidth, and damage morphology [10-15]. In liquids, similar threshold measurements have been made, and the dynamics of pressure wave propagation and cavitation have been studied [16-23]. However, no studies have been reported on the very early time dynamics following breakdown in any condensed matter system. In this paper, we present time-resolved imaging and time-resolved scattering techniques for observing these early time dynamics, and discuss measurements made in water. We find that the initial expansion of the laser-produced plasma is delayed by 20 ps, in spite of its high temperature. We attribute this delay to the electron-ion energy transfer time. In addition, we track the dynamics over eight orders of magnitude in time, from the initial excitation of the plasma to the final collapse of the cavitation bubble, providing the most complete picture obtained to date of the dynamics of femtosecond laser-induced breakdown in a liquid.

We study the interaction of intense ultrashort laser pulses with transparent materials, *i.e.* materials that do not normally absorb the laser radiation. When a femtosecond laser pulse is tightly focused inside a transparent material the intensity in the focal volume can become high enough to cause absorption through nonlinear processes [11-15]. Because the absorption is so strongly intensity dependent, it can occur at the focus inside the material while leaving the surface unaffected. Intially, most of the highly-excited free electrons created by the laser pulse remain confined to the micrometer-sized focal region because of the Coulomb attraction from

#685 - $15.00 US Received December 19, 2001; Revised February 08, 2002

the still undisturbed ions. Within tens of picoseconds, however, energy is transferred from the free electrons to the ions. The result is a micrometer-sized, highly-excited plasma, trapped inside the material. The hot plasma explosively expands into the surrounding material with a velocity exceeding the speed of sound.

We measure the dynamics of this explosive expansion using time-resolved imaging and scattering techniques. Imaging with a time-delayed laser pulse provides a direct view of the explosion dynamics, but, until now, has been limited to observing events on nanosecond and longer time scales because the spatial resolution of previous experiments was not sufficient to reliably image the early stages of the growth, when the plasma is small [16-18, 20, 22, 24, 25]. Time-resolved scattering provides an indirect measure of the plasma size that does not suffer from limited spatial resolution, but which requires more accurate knowledge about the plasma properties to properly interpret.

Pump-probe imaging

Fig. 1 shows the time-resolved imaging setup. A 100-fs, 800-nm wavelength pump pulse is focused by a 0.65 numerical aperture (NA) microscope objective into a water flow cell. The resulting dynamics are imaged onto a CCD camera with a time-delayed probe pulse. For short time delays, the probe pulse was a 100-fs duration, frequency doubled (400-nm wavelength) replica of the pump pulse, optically delayed with respect to the pump. For time delays longer than a few tens of nanoseconds we used an electronically triggered diode laser as the probe to avoid using long optical delay lines. The diode laser produces 100-ps pulses at a wavelength of 680 nm. The jitter between the pump and diode laser pulses is less than 10 ps. A spectral filter blocks the 800-nm pump pulse in both cases. A vibrating (~15 Hz) diffuser plate is used to reduce the speckle caused by the nearly monochromatic illumination of the probe pulse. The resolution limit of the imaging setup is approximately 4 μm, sufficient to resolve a bubble with a 2-μm radius.

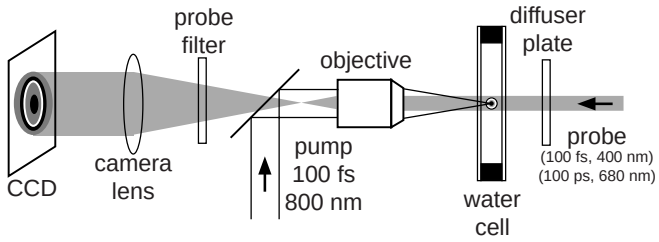

Fig. 1 Time-resolved imaging setup for observing the dynamics of laser-induced breakdown. A time-delayed probe pulse illuminates the dynamics induced by the femtosecond pulse. The objective used to focus the femtosecond pulse images the dynamics onto a CCD camera.

A sequence of images of the breakdown dynamics in water probed at various time delays after excitation by a 1-μJ pump pulse is shown in Fig. 2. A corresponding movie (linked from the figure caption) shows the first 10 ns of the expansion on a linear time scale (slowed down by 10^9). At 1 μJ, the laser pulse energy exceeds the optical breakdown energy threshold in water by about a factor of 10. At this energy, the volume where the laser intensity exceeds the threshold intensity is cone-shaped, with the tip of the cone located at the laser focus and the base extending toward the incident direction of the laser. The base of the cone is located a little over 1 μm upstream from the focus and has a radius of 0.5 μm. Because we image in a plane perpendicular to the beam propagation direction, we therefore expect to see the formation of a plasma with a 0.5-μm radius. The images shown in Figure 2 were obtained with the 400-nm, 100-fs probe. Each image is the average of 100 CCD photographs. The 25-ps image shows a small bubble formed at early times which, after a delay of tens of picoseconds, grows rapidly. At these early times, the bubble consists of an electron-ion plasma, which provides optical contrast through absorption, reflection, and refractive index

#685 - $15.00 US Received December 19, 2001; Revised February 08, 2002

change. The rapid growth of the plasma is evident from a comparison of the 25-ps and 100-ps images. The growth remains supersonic for a few hundred picoseconds, but by 400-ps is no longer supersonic, and all further dynamics occur at acoustic or slower velocities. In the 1.6-ns image we can begin to see the separation of an acoustic pressure wave from the central bubble. The pressure wave produces density variations in the water that translate to refractive index variations, providing the contrast seen in the figure [21]. By 6.4 ns, the acoustic wave is clearly separated, and the central bubble has not expanded significantly compared to the 400-ps image. Images obtained on a microsecond time scale using the diode laser probe show that the central bubble expands and re-collapses as a cavitation bubble (images not shown). At these long times, optical contrast is provided by the large refractive index difference between the water outside the bubble, and the vaporized material inside the bubble.

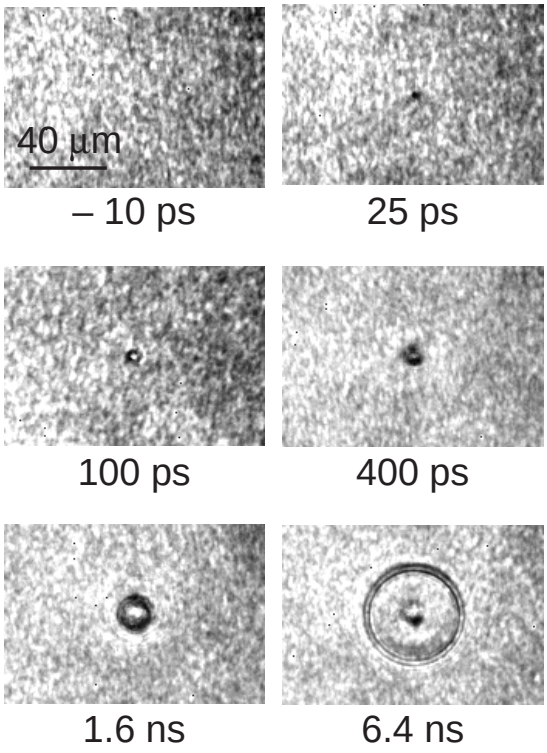

Fig. 2 Images of femtosecond laser-induced breakdown in water obtained for various time delays using the setup shown in Fig. 1. A corresponding quicktime movie shows the first 10 ns of expansion. One second of the movie shows 1 nanosecond of the dynamics.

Fig. 3 summarizes the results of the imaging measurements in water over eight orders of magnitude in time. The filled circles and open squares are the radii of the bubble and pressure wave, respectively, obtained from the images. The graph shows that a hot electron plasma with a radius of about 2 µm is formed within 200 fs. Note that this size is at our resolution limit, so the initial size could be smaller. Until about 20 ps after excitation, the radius remains constant or, at least, smaller than the resolution limit of the imaging system. Beginning at about 30 ps and continuing to 200 ps, there is a very rapid growth in the size of the plasma. After this rapid growth the radius begins to oscillate at a radius of about 6 µm. At about 800 ps, the images show that a pressure wave separates from the central bubble, and travels outward at the speed of sound in water (1.48 µm/ns). The central bubble maintains its nearly constant radius until about 10 ns, when it begins to expand as a cavitation bubble. The

#685 - $15.00 US Received December 19, 2001; Revised February 08, 2002

cavitation bubble reaches a maximum radius of 100 μm at 5 μs, and then re-collapses by 11 μs. In previous studies of ultrashort pulse-induced breakdown in water picosecond dynamics on the micrometer-scale were not resolved [16-18, 20, 22, 24, 25].

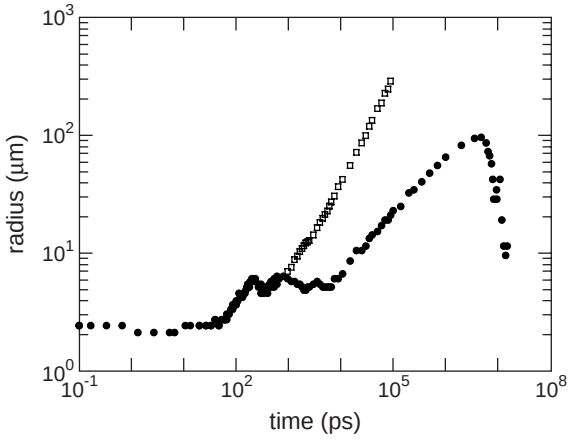

Fig. 3 Evolution of the radius of the laser-produced plasma, pressure wave, and cavitation bubble as a function of time (● plasma/bubble radius, ❑ pressure wave).

Time-resolved scattering

To better resolve the plasma radius at early times, we measured the light scattered from the laser-produced plasma using a pump-probe technique, illustrated in Fig. 4. The probe beam illuminates an area of about 30-μm diameter around the center of the pumped region in the sample. The directly transmitted probe beam is blocked, so that the detector registers only the light that is scattered out of the undisturbed beam path and travels around the beam block.

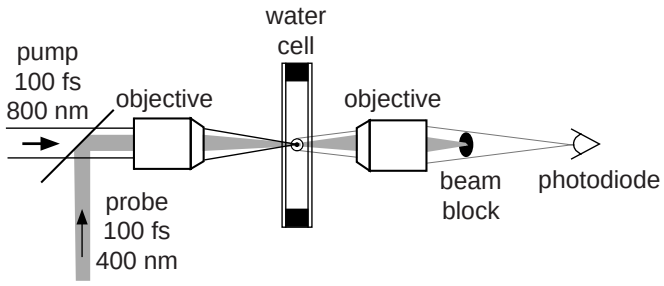

Fig. 4 Time-resolved scattering setup. The directly transmitted probe beam is blocked so that only scattered probe light reaches the detector.

Fig. 5 shows the time-resolved scattering signal from the plasma from 100 fs to 1 ns. Between 10 ps and 1 ns, the scattering signal shows similar features to the imaged radius shown in Fig. 3. The rise time of the scattering signal indicates that the plasma is formed within 200 fs. Because plasma formation should occur within the duration of the pump pulse, this 200-fs rise time serves as a characterization of the temporal resolution of the setup. We observe the same 20-ps delay before the scattering signal increases that we observe in the imaged radius. The increase in the scattering signal from 30 ps to 200 ps is very rapid, as for the imaged radius.

#685 - $15.00 US Received December 19, 2001; Revised February 08, 2002

The amplitude of the scattered signal depends on the size and density of the plasma. It is difficult to deconvolve these two dependencies without additional measurements. In particular, a measurement of the time-resolved transmission and reflection from the plasma would allow the plasma density as a function of time to be determined. With the plasma density known, the scattering signal would provide a measure of the plasma size, without the image resolution limits of the time-resolved imaging technique. If we assume that the plasma density is always above the critical density for the 400-nm probe light (about 10^{22} cm^{-3}), then the plasma acts like a metallic ball, and the scattered amplitude is proportional to the cross-sectional area of the plasma. We can then use the imaged radius from 100 ps to 1 ns to calibrate the scattering signal. The axis on the right of Fig. 5 shows the radius obtained using this procedure. The radius in the plateau region from 200 fs to 20 ps, at 0.8 μm, is smaller than that determined from the imaging experiment. This is consistent with the fact that the resolution of the imaging setup was not sufficient to resolve such a small plasma. The plasma size determined from the scattering data is slightly larger than the 0.5-μm radius calculated for 0.65 NA focusing and an energy that exceeds the threshold energy by a factor of 10. Spherical aberration could be responsible for this increase in focal spot size.

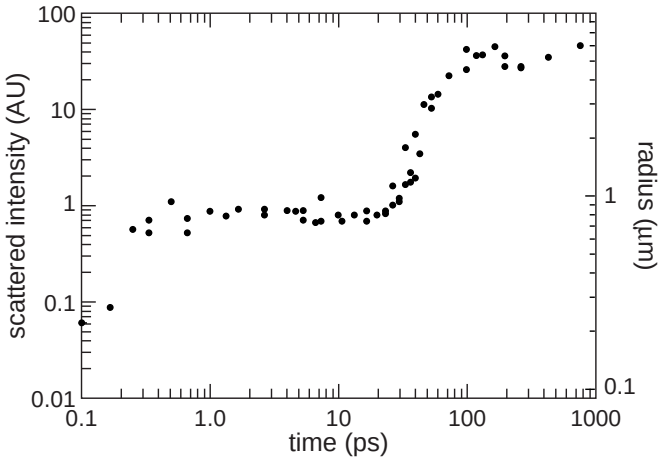

Fig. 5 Time-resolved scattering signal from femtosecond laser-induced breakdown in water. The scale on the right axis was calculated assuming the plasma density is always sufficiently high that the scattered intensity depends only on the cross-sectional area of the plasma. The imaged radius is then used to calibrate the scattering signal in the 100 ps to 1 ns region.

Discussion

Some features of the dynamics shown in Fig. 3 and Fig. 5 are easily explained. The laser-produced plasma is very hot compared to the surrounding material, so it tends to expand, doing work on the surrounding material. The plasma expansion stops when the kinetic energy of the plasma has been used up doing this work. As the plasma expansion stops, a pressure wave continues to propagate outward [18, 20]. From Figure 5, we see that this separation of the pressure wave occurs at about 800 ps. After about 10 ns, the electron-ion plasma recombines [24], and much of the ionization energy is converted to heat, leaving a hot gas-filled bubble which expands as a cavitation bubble, once again doing work on the surrounding material [26, 27]. The expansion stops and reverses as the gas cools. The 10-ns electron-ion recombination time is consistent with the lifetime of the plasma luminescence that we observe. The main observations that remain to be explained are the 20 ps delay before the size of the plasma begins to grow, the extremely rapid growth of the plasma radius from 30 ps to 200 ps, and the launch of the pressure wave at 800 ps even though the plasma growth seems to stop at 200 ps.

#685 - $15.00 US Received December 19, 2001; Revised February 08, 2002

The plateau in the radius from 200 fs to 20 ps indicates that the electron plasma produced by the laser pulse does not expand immediately after the excitation. We attribute this 20-ps delay to the electron-ion energy transfer time. Most of the electrons in the hot plasma cannot expand on their own because they do not have enough kinetic energy to overcome the electrostatic attraction of the cold ions. Once the electrons transfer sufficient kinetic energy to the ions, the hot ions and electrons move out of the focal region together, without charge separation. Similar electron-ion energy transfer times have been observed in semiconductors [28].

If we take the increase in size of the plasma from 30 ps to 200 ps to be due to physical expansion of the plasma produced by the laser pulse at the laser focus, we find an expansion velocity of 30 μm/ns, or 20 times the speed of sound in water. The pressure required to drive such a shock wave is on the order of 10 Gbar [21]. However, using the procedure outlined by Glezer in Ref. [10], we obtain an upper limit of 400 kBar on the pressure created under our experimental conditions, ruling out the possibility that the rapid plasma growth observed between 30 and 200 ps is due to expansion of the plasma produced in the focal volume by the laser pulse [29]. Furthermore, note that the pressure wave is not launched until 800 ps after excitation, after the bubble radius in Figure 3 goes through a small oscillation. If the rapid growth in radius from 30 ps to 200 ps were an expansion of the electron-ion plasma produced by the laser pulse, one would expect the pressure wave to be launched at the end of the expansion, not 600 ps later. Perhaps the expansion of the electron-ion plasma produced by the laser pulse takes 800 ps, and it launches the pressure wave when the expansion runs out of energy and stops. This expansion would have a velocity of about 5.2 μm/ns or 3.5 times the speed of sound in water. The pressure required to drive such a supersonic expansion is about 110 kBar [21], well within the upper limit mentioned above. It seems likely, then, that the expansion of the laser-produced plasma is much slower than the growth of the plasma size observed in the imaging and scattering experiments, and that the end of the growth of the laser-produced plasma is indicated by the launch of the pressure wave.

What then is responsible for the very rapid growth in the radius between 30 and 200 ps? Most likely, some mechanism induces plasma formation outside the focal volume. One possibility is that the ultraviolet component of the radiation emitted by electron-ion recombination in the laser-produced plasma ionizes material outside the focal region. Alternatively, ballistic transport of the very high energy tail of the electron distribution produced by the laser pulse out of the focal volume could lead to dense plasma formation outside the irradiated region. Rough calculations [29] show that the highest energy 0.01% of the electron distribution can expand approximately 5 μm out from the focal volume into the surrounding material against the Coulomb attraction from the ions. Because of their high energy, each of these electrons could ionize another 250 electrons outside the focal volume via. impact ionization, leading to a plasma density on the order of 10^{19} cm^{-3} in a 5-μm radius volume around the laser focus, which we could perhaps detect [30]. Either this ballistic electron transport or the ultraviolet ionization would happen much faster than the expansion of the laser-produced electron-ion plasma, explaining the very rapid growth observed between 30 ps and 200 ps. One would also not expect the ballistic electrons nor electrons produced by ultraviolet or avalanche ionization outside the focal volume to launch a pressure wave, which is consistent with our observations. Additional measurements and theoretical work is necessary to fully explain the rapid plasma growth we observe from 30 ps to 200 ps.

Conclusions

The ultrafast laser-induced optical breakdown described in this report opens the door to a number of interesting new opportunities. Using a relatively simple femtosecond laser it is possible to carry out tabletop studies of confined, high-density, high-temperature plasmas. Because femtosecond laser-induced optical breakdown requires less energy and produces more confined damage than optical breakdown with longer pulses, it may find promising applications in ophthalmology, in retinal microsurgery, and in medical and biological experiments [6, 31]. As shown in Fig. 3, the region of supersonic expansion is limited to a 7-

#685 - $15.00 US Received December 19, 2001; Revised February 08, 2002

μm radius for 1-μJ, 100-fs pulses. In contrast, supersonic expansion over several hundred micrometers is often observed with breakdown induced with picosecond laser pulses [21]. Because this supersonic expansion causes collateral tissue damage, femtosecond pulses offer much higher surgical precision. Recently, femtosecond pulses have been used to perform single-cell and sub-cellular surgery [7, 8]. Finally, in solids the breakdown leaves behind a permanently damaged region inside the material which can be used for micromachining [1-4].

Acknowledgments

This work was funded by the National Science Foundation.

#685 - $15.00 US Received December 19, 2001; Revised February 08, 2002